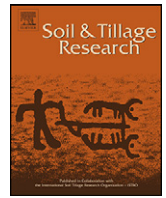


Contents lists available at [SciVerse ScienceDirect](http://www.sciencedirect.com)

Soil & Tillage Research

journal homepage: www.elsevier.com/locate/still

Non-invasive field measurements of soil water content using a pulsed 14 MeV neutron generator

S. Mitra^{a,*}, L. Wielopolski^a, R. Omonode^b, J. Novak^c, J. Frederick^d, A.S.K. Chan^e

^a Environmental Sciences Department, Brookhaven National Laboratory, Upton, NY 11973, United States

^b Department of Agronomy, Purdue University, West Lafayette, IN 47907, United States

^c USDA-ARS, USDA-ARS-Coastal Plains Research Center, 2611 W. Lucas Street, Florence, SC 29501-1241, United States

^d Clemson University, Pee Dee Research & Education Center, 2200 Pocket Road, Florence, SC 29506-9706, United States

^e Collaborator, USDA-ARS, National Laboratory for Agriculture and the Environment, 2110 University Boulevard, Ames, IA 50011-3120, United States

ARTICLE INFO

Article history:

Received 8 July 2010

Received in revised form 30 December 2011

Accepted 31 December 2011

Available online 26 January 2012

Keywords:

Non-invasive measurement

Soil water

Field studies

Pulsed 14 MeV neutrons

Prompt gamma-ray

ABSTRACT

Current techniques of soil water content measurement are invasive and labor-intensive. Here, we demonstrate that an in situ soil carbon (C) analyzer with a multi-elemental analysis capability, developed for studies of terrestrial C sequestration, can be used concurrently to non-invasively measure the water content of large-volume (~0.3 m³) soil samples. Our objectives were to investigate the correlations of the hydrogen (H) and oxygen (O) signals with water to the changes in the soil water content in laboratory experiments, and in an agricultural field. Implementing prompt gamma neutron activation analyses we showed that in the field, the signal from the H nucleus better indicates the soil water content than does that from the O nucleus. Using a field calibration, we were able to use the H signal to estimate a minimum detectable change of ~2% volumetric water in a 0–30 cm depth of soil.

Published by Elsevier B.V.

1. Introduction

Knowledge of soil water content is critical to agricultural, hydrological and meteorological researches. Soil moisture–climate interactions are increasingly of interest in a changing climate, as recently reviewed by (Seneviratne et al., 2010). For example such data are vital for understanding the soil's hydraulic properties that are essential input to most hydrologic and climate models (Ines and Mohanty, 2008), because soil moisture is linked to evaporation and thus to the distribution of heat fluxes from the land to the atmosphere. Soil water sensors routinely are used in applications such as research on crop production, water budgeting in water sheds, precision agriculture and irrigation scheduling. Earlier, Schmugge et al. (1980) surveyed methods used to determine soil moisture content which included gravimetric, nuclear, electromagnetic and remote sensing techniques. Their study also included tensiometric techniques for measuring soil water potential that describes the energy status of the soil water and is an important parameter for water transport analyses, water storage estimates and soil–plant–water relationships. A recent review by Robinson et al. (2008) highlights the need for bridging the gap between point scale measurements (<1 m²) and obtaining areal averages (10–

100 m²) that are necessary for spatial data describing watershed patterns. They discussed several emerging methods and technologies from geophysics such as ground penetrating radar and electromagnetic induction, together with some approaches for obtaining better spatial coverage that use time domain reflectometers (TDRs) fitted on mobile platforms like tractors and all-terrain vehicles (ATVs). However, these sensors are invasive and do not possess on-the-go sensing capabilities.

Here, we discuss the feasibility of extending the functionality of a surface nuclear probe that primarily was designed for non-invasive, in situ measurements for monitoring and verifying the soil's carbon stocks resulting from carbon-sequestration programs (Wielopolski et al., 2008, 2011). In this technique, fast neutrons produced by an electrically switchable pulsed 14 MeV neutron generator (NG) impinge on the soil and interact with its various elements. During the neutron burst (the ON state of the NG) they undergo inelastic neutron scattering (INS) with C and O nuclei; between the bursts (the OFF state of the NG), the neutrons previously released during the ON state, slow down via elastic scattering with the soil's matrix elements, particularly H, so that eventually some are captured in a thermal neutron capture (TNC) process. It is expected that the density of the resultant cloud of slow neutrons and the intensity of the characteristic 2.22 MeV prompt capture gamma-rays from H will be a function of the soils' water-content. To the best of our knowledge, there are no earlier reports of measuring neutron-induced prompt gamma-ray signals

* Corresponding author. Tel.: +1 631 344 6377; fax: +1 631 344 2060.
E-mail address: smitra@bnl.gov (S. Mitra).

from H and O as a direct method to determine soil water under field conditions. The proposed method is quite distinct from the commercial neutron probe that measures soil moisture indirectly by detecting the thermalized neutrons escaping the soils' matrix.

Our objectives were the following:

- Demonstrate, in laboratory experiments, the response of the H and O signals from the surface nuclear probe to linear changes in the soil's moisture content.
- Compare the response of our instrument to changes in the water content of an agricultural field with that of the conventional theta-probe technique and to volumetric determination from soil cores.

2. Materials and methods

The instrument was assembled and mounted on a cart at Brookhaven National Laboratory (BNL), New York (Fig. 1). Static measurements can be acquired at a fixed spot, or the cart can be towed across a field in the scan mode to integrate the data across a field. The system consists of a pulsed 14 MeV NG and three 12.7 cm × 12.7 cm × 15.2 cm NaI(Tl) gamma-ray detectors whose signal outputs are summed and processed on board by a digital multi-channel analyzer (MCA) that concurrently records an INS- and TNC-spectrum in real time (Mitra et al., 2007). The NG and gamma-ray detectors are positioned 25 cm above the soil's surface. All instrumental-runs take an hour. Net elemental yields (net peak-area counts), were obtained by subtracting a background area from the total area in a region of interest of the gamma-ray spectrum, using the trapezoidal method (Wielopolski et al., 2008).

2.1. Laboratory and field experiments

Laboratory experiments were conducted at the Soil Analysis Facility at BNL, using topsoil collected from a nearby forest within the BNL campus. The soil was well drained Riverhead sandy loam (coarse-loamy, mixed, active, mesic Typic Dystrudepts), with 0–3 percent slopes. The soil was spread out in a barn with adequate ventilation and allowed to air-dry for about 3 weeks before being used for determining selected soil characteristics. The dried forest soil was screened through a 2 mm mesh to remove roots and other undesired debris before being used for laboratory measurements; thus all laboratory experiments were performed using disturbed topsoil. Similarly, prior to commencement of the experiments, the amount of the dry and sieved topsoil that was needed to fill the

experimental pit (dimension 1.52 m × 1.52 m × 0.5 m deep) was determined to be ~1.0 Mg (1000 kg).

Triplicate subsamples of the sieved soil were collected and used to estimate the water holding and bulk density characteristics. Maximum soil-moisture holding capacity was estimated by tightly packing the air-dried soil into column (Teflon-stopcock and fritted disc columns; inner diameter = 22 and length = 300 mm) and a known quantity of water was gradually added from the top of the column until the soil was fully saturated (when the first few drops of water seeped out of the column). Although we are aware of the hysteresis effect, adding water to the soil column was more convenient to accurately determine the amount of water being added to the soil columns. In the absence of pressure plates, we estimated the soil's field water holding capacity (FC) by allowing the soil to drain for 24–48 h after adding the water to achieve maximum soil capacity; we assumed that this time frame was adequate for the soil macro pores to drain. Thereafter, the amount of water needed to bring the soil up to 25, 50, and 75% of the FC was calculated. Bulk density values also were determined in triplicates by filling aluminum cans of known volume (diameter, 7.6 cm and depth, 5.4 cm) with the soil, weighed, oven dried and re-weighed after drying to a constant weight at 105 °C for 24–48 h.

The relationship between the different soil water contents and the H and O signals were determined at 0, 25, 50 and 75% of the FC by adding the pre-determined amounts of water needed to bring the 1.0 Mg of soil to these desired soil water contents. Briefly, after recording the H and O signals in triplicate by centering the instrument on the pit, the soil was evacuated from the pit into a mechanical mixer and the desired amount of water was added to bring its soil water content to the next higher FC. After thorough mixing, the soil immediately was transferred back into the pit, and the H and O signals were recorded again. This cycle was repeated to cover the range of soil water up to 75% FC. At each soil water holding capacity level (0, 25, 50 and 75% FC), soil samples were collected in triplicate at random locations in the pit before and after the instrumental runs and gravimetrically estimated for the true water content levels. Unfortunately, the H and O measurement was not performed at maximum water holding capacity due to an apparent breakdown of the soil after repeated mixing.

Field experiments were carried out at the Clemson University Pee Dee Research and Education Center, Darlington, South Carolina. The INS and TNC spectra were recorded at seven fixed locations within a field along an approximately 100 m long transect situated up-slope to down-slope that corresponded with the soil mapping units shown in Fig. 2. This field is comprised of well-drained soils in up-slope positions with poorly drained soils located in depression areas. The latter soils areas are depicted as circular patterns referred to as Carolina Bays (Daniels et al., 1999). Field locations progressively up-slope consisted of grid points labeled V12, W11, Y11 and AB10 respectively. These up-slope soil series are well drained soils and had topsoil dominated by sand. Field locations progressively down-slope were labeled T12, S12 and S13, respectively. Soils in these locations are poorly drained and frequently received eroded silt and clay causing the top soil to have lower sand contents (Novak et al., 2009). The field has been under cultivation with row crops (corn, soy bean and cotton) for the past 20 years. Table 1 summarizes selected soil characteristics of the field.

At each location, and within the nuclear probe's footprint of ~150 cm diameter, we measured (a) volumetric content of soil moisture to a depth of 6.5 cm with a factory calibrated, Dynamax, TH₂O portable soil moisture theta probe at three spots before and after the INS measurements, and, (b) gravimetrically analyzed soil water from five cores collected within a 1 m² area centered on the instrument's footprint, using a soil probe with inner diameter of 3.12 cm. Each core was subsequently subdivided into 0–5, 5–10, 10–20, 20–30 and 30–40 cm depth intervals, bagged and taken to

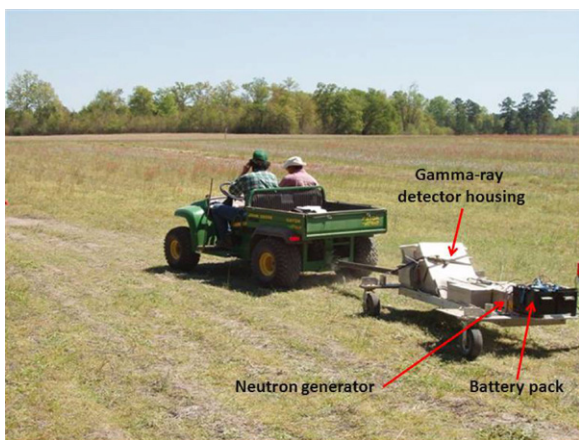


Fig. 1. The mobile nuclear probe built at Brookhaven National Laboratory comprises a 14 MeV pulsed neutron generator and three NaI(Tl) gamma-ray detectors that detect the Hydrogen and Oxygen signals. All on-board instruments are powered by a 12 V battery.

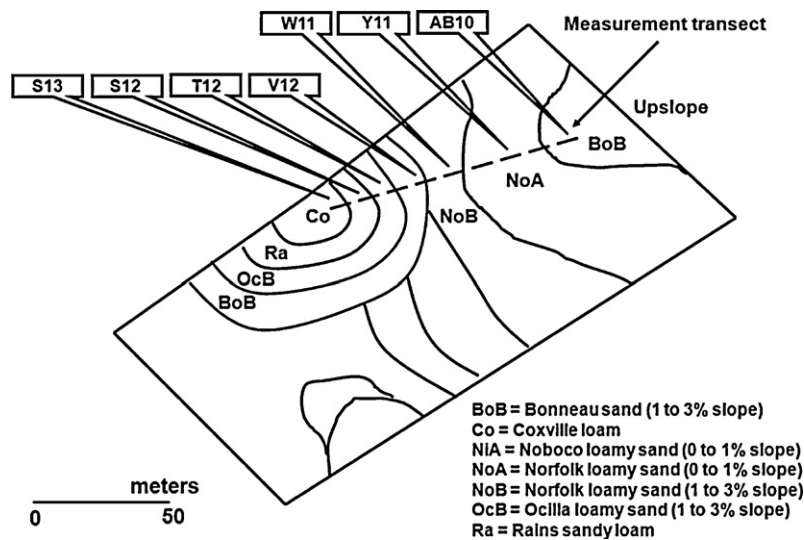


Fig. 2. Soil moisture measurement locations at the Pee Dee Research and Education Center, SC. The bands represent soil series mapped across the field as identified by Novak et al. (2009).

the laboratory for analysis. Gravimetric soil water content and bulk density was estimated for each depth interval by weighing fresh soil and re-weighing them after oven drying at 105 °C to a constant weight. The volumetric soil water content for any depth was obtained by multiplying the corresponding thermogravimetry data with the soil bulk density for each depth interval.

3. Results and discussion

3.1. Laboratory tests

Selected soil characteristics determined for the Riverhead sandy loam topsoil gave a bulk density value of $1.02 \pm 0.01 \text{ g cm}^{-3}$, while the maximum water holding capacity and field capacity respectively were ~ 366 and 209 g kg^{-1} soil. The gravimetric soil water content estimated for this soil was 52, 105 and 157 g kg^{-1} soil at 25, 50 and 75% FC, correspondingly.

Fig. 3 shows the H and O yields obtained for a 1 h laboratory assessment of this same topsoil at different water contents. The yields of both increased linearly, exhibiting high correlations with increasing water content ($r^2 = 0.94$ for O and 0.98 for H). It is suspected that the high intercepts for O and H reflect the instrumental background from the water tanks that are used for radiobiological shielding against neutrons.

3.2. Field tests

Tables 2 and 3 summarize the mean volumetric water content and bulk densities averaged over 5 cores at different depth

Table 1

Selected soil characteristics at the Clemson University Pee Dee Research and Education Center (particle sizes are mean values with a relative error of $0.5\% \text{ w w}^{-1}$).

Series	Depth (cm)	Sand (%)	Silt (%)	Clay (%)	Texture
Bonneau	0–15	87.0	11.0	2.0	Sand
Coxville	0–15	44.5	45.0	10.5	Sand
	20–40	55.0	23.9	21.1	Sandy clay loam
Noboco	0–15	80.0	17.5	2.5	Loamy sand
Norfolk	0–15	82.5	15.5	2.0	Loamy sand
	15–35	65.1	30.4	4.5	Sandy loam
Ocilla	0–15	82.5	14.5	3.0	Loamy sand
Rains	0–15	60.0	33.0	7.0	Loamy sand

Particle sizes (mm): Sand: 2.0–0.05, Silt: 0.05–0.02, Clay: <0.002 .

intervals. In general, water content increased with depth at each location, either up-slope (well drained) or down-slope (poorly drained) mainly due to the gravitational downward movement of water. The volumetric soil water profile in the subsurface is illustrated in Fig. 4. Plotting the gamma-ray yields against the volumetric water content revealed the best linear relationship ($r^2 = 0.99$) between H yield and water content for cores taken at depths from 10–20 cm (Fig. 5), a finding consistent with the Monte Carlo simulation data of Shue et al., 1998. They found that for a point isotropic source of 14 MeV neutrons located 15 cm above the surface of soil, the maximum thermal-neutron flux occurred at a depth from 10 to 20 cm. Since the H signal intensities are directly proportional to the thermal neutron flux, the maximum intensities are expected from this depth. The fits for H are less well correlated at shallow depths to 10 cm due to insufficient thermalization of the neutrons; thermalization of the incident neutron's energy progresses going down from the surface. If needed, a thermalizer could be introduced between the NG and soil to shift the thermal neutron flux to the shallow depths. However, the system is less responsive to changes in O that reflect changes in the soil's water content

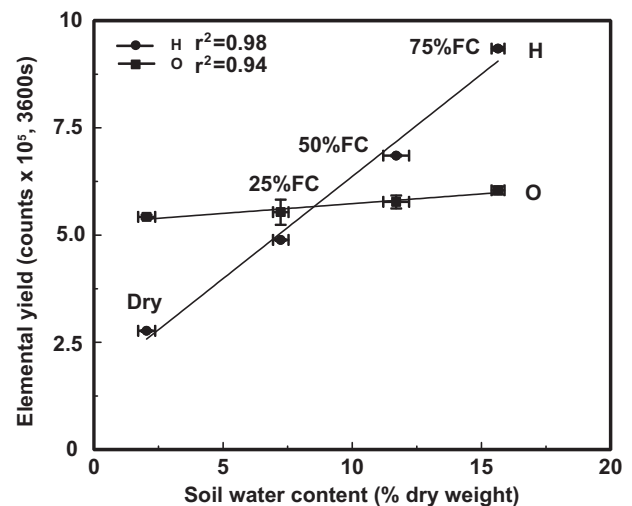


Fig. 3. The linear relationship of the neutron probe's H and O yields with gravimetrically determined soil water content in laboratory tests. The data are from Riverhead sandy loam top soil.

Table 2
Mean volumetric water content and bulk density (\pm standard deviation), of the 5 cm thick bands at different soil depths at each field location of the Pee Dee Research and Education Center, SC. The bulk density values are presented within parentheses.

Depth (cm)	Mean water content ($\text{m}^3 \text{m}^{-3}$), (bulk density, g cm^{-3})							
	S13	S12	T12	V12	W11	Y11	AB10	
0–5	0.053 \pm 0.007 (1.49 \pm 0.09)	0.057 \pm 0.015 (1.47 \pm 0.13)	0.009 \pm 0.006 (1.40 \pm 0.16)	0.041 \pm 0.029 (1.49 \pm 0.22)	0.073 \pm 0.049 (1.47 \pm 0.11)	0.026 \pm 0.026 (1.57 \pm 0.12)	0.013 \pm 0.009 (1.53 \pm 0.23)	
5–10	0.085 \pm 0.013 (1.53 \pm 0.18)	0.077 \pm 0.021 (1.57 \pm 0.11)	0.022 \pm 0.010 (1.61 \pm 0.14)	0.040 \pm 0.008 (1.60 \pm 0.07)	0.056 \pm 0.013 (1.65 \pm 0.08)	0.011 \pm 0.009 (1.56 \pm 0.07)	0.022 \pm 0.011 (1.65 \pm 0.17)	
10–20	0.129 \pm 0.008 (1.69 \pm 0.07)	0.084 \pm 0.005 (1.63 \pm 0.02)	0.044 \pm 0.008 (1.60 \pm 0.07)	0.074 \pm 0.004 (1.72 \pm 0.06)	0.065 \pm 0.013 (1.68 \pm 0.03)	0.051 \pm 0.011 (1.67 \pm 0.07)	0.071 \pm 0.009 (1.77 \pm 0.08)	
20–30	0.135 \pm 0.010 (1.73 \pm 0.07)	0.089 \pm 0.012 (1.72 \pm 0.06)	0.089 \pm 0.012 (1.77 \pm 0.06)	0.082 \pm 0.004 (1.78 \pm 0.04)	0.059 \pm 0.020 (1.86 \pm 0.13)	0.076 \pm 0.027 (1.81 \pm 0.05)	0.071 \pm 0.010 (1.79 \pm 0.13)	
30–40	0.104 \pm 0.026 (1.47 \pm 0.11)	0.113 \pm 0.018 (1.37 \pm 0.12)	0.094 \pm 0.024 (1.41 \pm 0.21)	0.102 \pm 0.029 (1.69 \pm 0.29)	0.060 \pm 0.002 (1.75 \pm 0.20)	0.058 \pm 0.023 (1.72 \pm 0.06)	0.047 \pm 0.014 (1.63 \pm 0.29)	

Table 3
Mean volumetric water content and bulk density (\pm standard deviation), for different depth intervals at the Pee Dee Research and Education Center, SC. The bulk density values are presented within parentheses.

Depth (cm)	Mean water content ($\text{m}^3 \text{m}^{-3}$), (bulk density, g cm^{-3})							
	S13	S12	T12	V12	W11	Y11	AB10	
0–5	0.053 \pm 0.007 (1.49 \pm 0.09)	0.057 \pm 0.015 (1.47 \pm 0.13)	0.009 \pm 0.006 (1.40 \pm 0.16)	0.041 \pm 0.029 (1.49 \pm 0.22)	0.073 \pm 0.049 (1.47 \pm 0.11)	0.026 \pm 0.026 (1.57 \pm 0.12)	0.013 \pm 0.009 (1.53 \pm 0.23)	
0–10	0.069 \pm 0.016 (1.51 \pm 0.14)	0.067 \pm 0.009 (1.52 \pm 0.13)	0.016 \pm 0.005 (1.51 \pm 0.18)	0.040 \pm 0.002 (1.55 \pm 0.17)	0.064 \pm 0.009 (1.56 \pm 0.13)	0.019 \pm 0.007 (1.56 \pm 0.09)	0.018 \pm 0.004 (1.58 \pm 0.21)	
0–20	0.089 \pm 0.030 (1.57 \pm 0.15)	0.073 \pm 0.011 (1.56 \pm 0.12)	0.025 \pm 0.014 (1.54 \pm 0.16)	0.052 \pm 0.016 (1.61 \pm 0.016)	0.065 \pm 0.007 (1.59 \pm 0.12)	0.029 \pm 0.017 (1.60 \pm 0.10)	0.035 \pm 0.025 (1.64 \pm 0.20)	
0–30	0.10 \pm 0.03 (1.61 \pm 0.15)	0.077 \pm 0.012 (1.60 \pm 0.13)	0.040 \pm 0.030 (1.59 \pm 0.17)	0.059 \pm 0.019 (1.65 \pm 0.16)	0.064 \pm 0.006 (1.66 \pm 0.17)	0.041 \pm 0.025 (1.65 \pm 0.13)	0.044 \pm 0.027 (1.68 \pm 0.19)	
0–40	0.10 \pm 0.03 (1.58 \pm 0.15)	0.084 \pm 0.018 (1.55 \pm 0.16)	0.052 \pm 0.034 (1.56 \pm 0.19)	0.068 \pm 0.024 (1.66 \pm 0.19)	0.063 \pm 0.006 (1.68 \pm 0.18)	0.045 \pm 0.023 (1.67 \pm 0.12)	0.045 \pm 0.024 (1.67 \pm 0.22)	

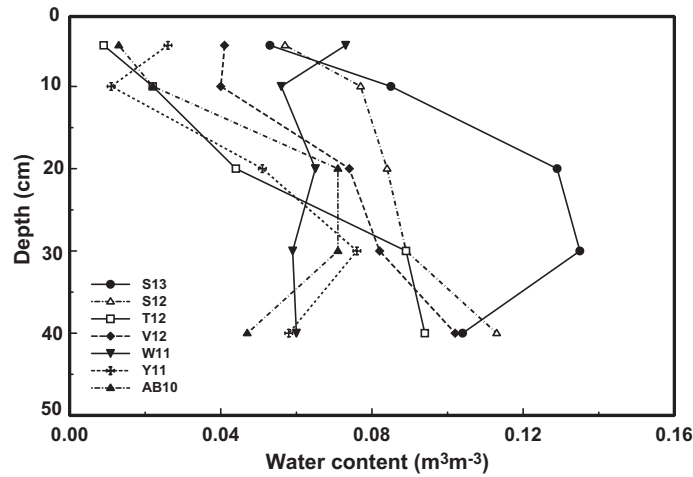


Fig. 4. Volumetric determination of soil water profile in the sub-surface at different measurement locations in the Pee Dee Research and Education Center, SC. S13 = Coxville; S12 = Raines; T12 = Ocilla; V12 = Bonneau–Ocilla; W11 = Norfolk B; Y11 = Norfolk A; and AB10 = Bonneau soil series.

because of the large background from the soil's O content. In addition, the O signal occurs for a threshold neutron energy value of about 6 MeV and the signal's intensity expectedly drops with depth as the neutron loses energy below 6 MeV due to collisions with the soil's matrix.

As a surface probe, the H yield best predicts soil water to depths of 30 cm ($r^2 = 0.89$, Fig. 6a). Fig. 6b illustrates the poor response of the O signals to the mean volumetric water content for the same 0–30 cm depth ($r^2 = 0.33$). Using the field moisture data for 0–30 cm depths, a linear regression equation relating soil water to H yield resulted in Eq. (1), where: Y = water content ($m^3 m^{-3}$) and X = hydrogen yield (counts h^{-1}),

$$Y = 2.1 \cdot 10^{-7}X - 0.0207, \quad r^2 = 0.89 \quad (1)$$

Based on a Poisson distribution for a single determination, the statistical variability, σ_{NetH} , of the net H gamma-ray yield at any location was estimated as:

$$\sigma_{NetH} = \sqrt{(T + B)} \quad (2)$$

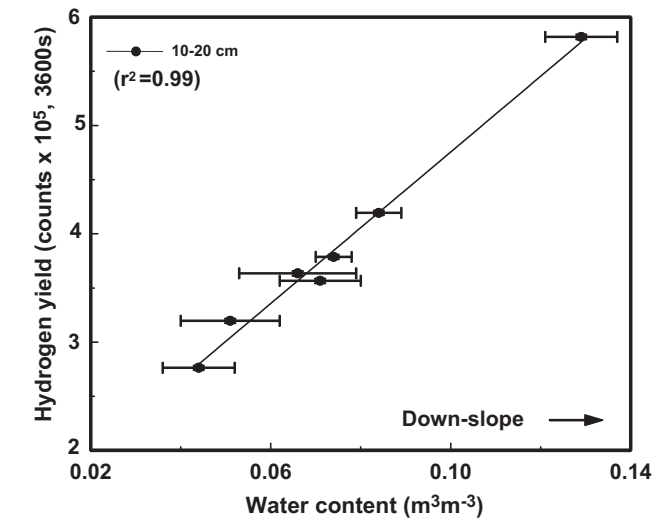
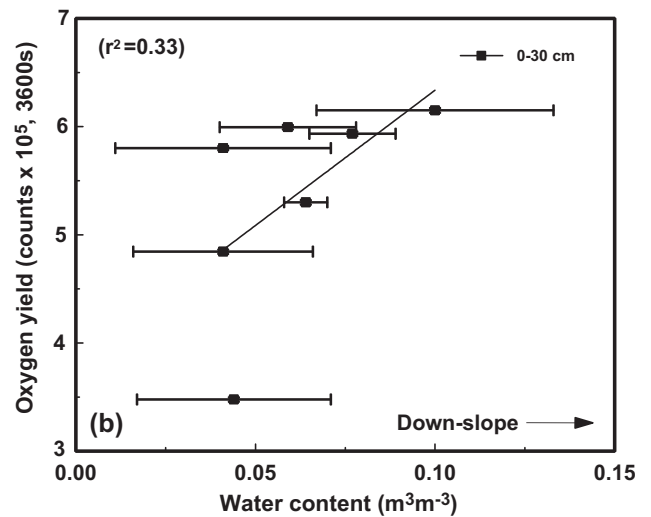
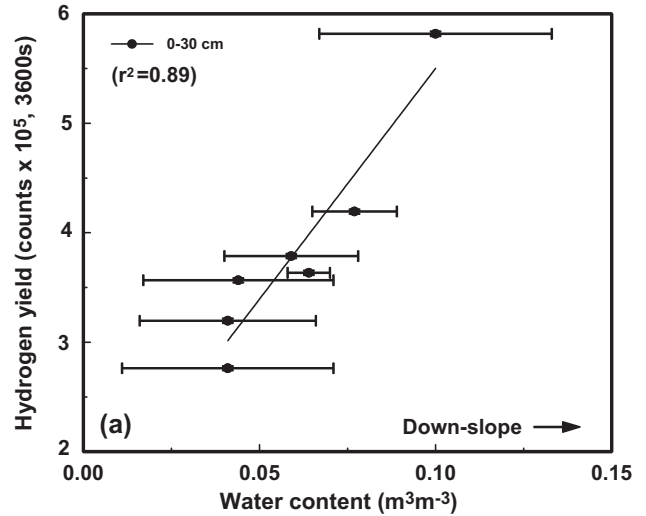


Fig. 5. H yield correlations with volumetric water content at 10–20 cm depth at different field locations in the Pee Dee Research and Education Center, SC. The down-slope arrow indicates a concomitant increase of soil water upon moving from up-slope to down-slope locations.

Fig. 6. Relationship of the gamma-ray yields with mean water content for 0–30 cm depth for (a) H, and (b) O at different field locations in the Pee Dee Research and Education Center, SC. The down-slope arrow indicates a concomitant increase of soil water upon moving from up-slope to down-slope locations.

Table 4

Coefficients of regression, r^2 , for linear regressions between mean volumetric water content at different depths and the H and O yields at each location in the Clemson University Pee Dee Research and Education Center (Darlington, SC).

Depth (cm)	r^2	
	H	O
0–5	0.28	0.22
5–10	0.70	0.35
10–20	0.99	0.11
20–30	0.62	0.29
30–40	0.20	0.36
0–10	0.55	0.32
0–20	0.79	0.27
0–30	0.89	0.33
0–40	0.80	0.49

where T and B are, respectively, the total and background counts under the H peak. The variability, σ_{NetH} , was $\sim\pm 2000$ counts (0.5%). Considering a $3\sigma_{\text{NetH}}$ change in the net number of counts as the minimum detectable change, it corresponds to $\sim 2\%$ change in the water content.

Table 4 summarizes the coefficients of regression, r^2 , for linear regressions between the H and O gamma-ray yields and the mean volumetric water content of the 5 cores at different depths. The poor correlations between the O yield and the mean volumetric water content at any depth is evident.

3.2.1. Comparison between the nuclear and the theta-probe method

As we concluded in the previous section, although the H yield of the nuclear probe best predicts the soil's volumetric water content, at depths between 10 and 30 cm compared with the gravimetric data, we thought it worthwhile to compare the data from the nuclear probe with the water content data obtained with the commonly used theta-probe technique. Despite the nuclear instrument being less sensitive to surface water between 0 and 10 cm depths because of insufficient thermalization of the fast neutrons, we nevertheless obtained a linear relation between the H yield and the volumetric water content predicted by the theta-probe down to 6.5 cm on moving from the up-slope

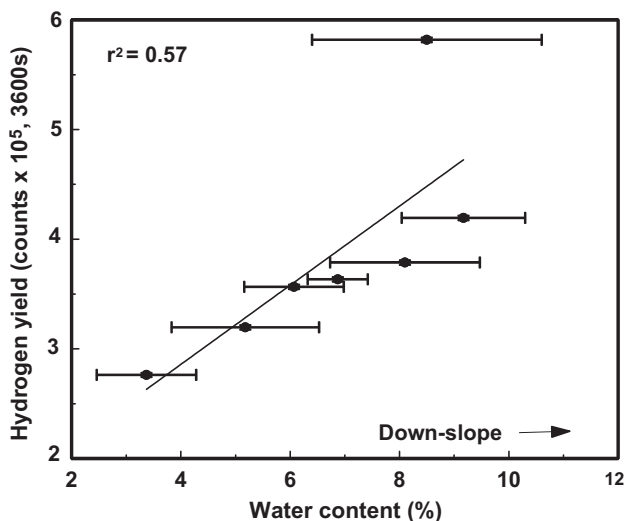


Fig. 7. Results of the linear regressions between H yields measured by the nuclear probe and the volumetric water content predicted by the theta-probe technique (0–6.5 cm depth) at different field locations in the Pee Dee Research and Education Center, SC. The down-slope arrow indicates a concomitant increase of soil water upon moving from up-slope to down-slope locations.

to down-slope regions (Fig. 7). As discussed earlier, the mean water content at any depth (Tables 2 and 3) was greater in the down-slope location than at up-slope locations. The variability not explained by these relationships could reflect the fact that the data from the nuclear- and theta-probes- did not represent the same volume at any given location; the nuclear probe samples much larger volumes ($\sim 0.3 \text{ m}^3$) than does the theta probe. Coupled to this, there was a 20% difference in soil water content at a measurement location determined from replicates using the theta probe.

4. Conclusions

Using pulsed 14 MeV neutrons to assess the soil water content in an agricultural field, and correlating the findings with the results for volumetric water determined gravimetrically from core samples, we demonstrated that we could non-invasively determine water content to a depth of 30 cm by measuring thermal neutron induced capture gamma-rays from H. On the other hand, the O signals correlated poorly with the soil's water content. This finding was in contrast to the excellent laboratory correlation of the H and O signals to linear changes in their respective concentrations in a homogenized soil matrix. Although the laboratory results proved that the H and O signal intensities rose with increasing soil water content, field standardization is necessary to calibrate the neutron probe to account for the heterogeneity of soil water content. Using the field data for such a calibration, this study indicates that the 14 MeV neutron probe can register a minimum detectable change in soil water of $\sim 2\%$ in a 0–30 cm depth of soil. The benefits of the mobile nuclear probe, is that a large tract of land can be non-destructively measured in a day and repeated measurements of large soil volumes can be undertaken readily. Accordingly, this technology potentially will deliver a quick, and more reliable mean profile from a field or plot that could be useful for assessing crop water use compared to the gravimetric, time-domain reflectometry, and capacitance probes that sample much smaller volumes. The probe has a switchable neutron source, and therefore, is radiologically safer for storage and transport than current soil moisture sensors that use radioactive neutron sources.

Acknowledgements

This manuscript has been co-authored by employees of Brookhaven Science Associates, LLC, under contract No. DE-AC02-98CH10886 with the U.S. Department of Energy. The United States Government retains, and the publisher, by accepting the article for publication, acknowledges, a world-wide license to publish or reproduce the published form of this manuscript, or allow others to do so, for the United States Government purposes. We gratefully acknowledge Dr Oded Doron's and Mr Don Watt's help with the logistics for field measurements at the Clemson University Pee Dee Research and Education Center (Darlington, SC).

References

- Daniels, R.B., Buol, S.W., Kleiss, H.J., Ditzler, C.A., 1999. Soil Systems in North Carolina. Tech. Bull. 314. North Carolina State Univ., Raleigh, NC.
- Ines, A.V.M., Mohanty, B.P., 2008. Near-surface soil moisture assimilation for quantifying effective soil hydraulic properties under different hydroclimatic conditions. *Soil Sci. Soc. Am. J.* 72 (1), 39–52.
- Mitra, S., Wielopolski, L., Tan, H., Fallu-Labruyere, A., Hennig, W., Warburton, W.K., 2007. Concurrent measurement of individual gamma-ray spectra during and between fast neutron pulses. *IEEE Trans. Nucl. Sci.* 54 (1), 192–196.
- Novak, J.M., Frederick, J.R., Bauer, P.J., Watts, D.W., 2009. Rebuilding organic carbon contents in coastal plain soils using conservation tillage systems. *Soil Sci. Soc. Am. J.* 73 (2), 622–629.

- Robinson, D.A., Campbell, C.S., Hopmans, J.W., Hornbuckle, B.K., Jones, S.B., Knight, R., Ogden, F., Selker, J., Wendroth, O., 2008. Soil moisture measurement for ecological and Hydrological Watershed-scale observatories: a review. *Soil Sci. Soc. Am. J.* 72 (1), 358–389.
- Schmugge, T.J., Jackson, T.J., McKim, H.L., 1980. Survey of methods for soil moisture determination. *Water Resour. Res.* 16, 961–979.
- Seneviratne, S.I., Corti, T., Davin, E.L., Hirschi, M., Jaeger, E.B., Lehner, I., Orlowsky, B., Teuling, A.J., 2010. Investigating soil moisture-climate interactions in a changing climate: a review. *Earth Sci. Rev.* 99, 125–161.
- Shue, S.L., Faw, R.E., Shultis, J.K., 1998. Thermal-neutron intensities in soils irradiated by fast neutrons from point sources. *Chem. Geol.* 144, 47–61.
- Wielopolski, L., Hendrey, G., Johnsen, K.H., Mitra, S., Prior, S.A., Rogers, H.H., Torbert, H.A., 2008. Nondestructive system for analyzing carbon in the soil. *Soil Sci. Soc. Am. J.* 72 (5), 1269–1277.
- Wielopolski, L., Chatterjee, A., Mitra, S., Lal, R., 2011. In situ determination of soil carbon pool by inelastic neutron scattering: comparison with dry combustion. *Geoderma* 160, 394–399.